

## Highly Luminescent Self-Organized Sub-2-nm EuOF Nanowires

Ya-Ping Du,<sup>†</sup> Ya-Wen Zhang,<sup>\*,†</sup> Zheng-Guang Yan,<sup>‡</sup> Ling-Dong Sun,<sup>†</sup> and Chun-Hua Yan<sup>\*,†</sup>

*Beijing National Laboratory for Molecular Sciences, State Key Laboratory of Rare Earth Materials Chemistry and Applications & PKU-HKU Joint Laboratory in Rare Earth Materials and Bioinorganic Chemistry, Peking University, Beijing 100871, China, and Microstructure & Properties of Advanced Materials, Beijing University of Technology, Beijing 100022, China*

Received September 21, 2009; E-mail: yan@pku.edu.cn; ywzhang@pku.edu.cn.

Inorganic nanostructures with one dimension approaching sub-2-nm and even one unit cell size possess unique chemical and physical properties and, thus, have drawn rapidly growing interest both fundamentally and technologically.<sup>1</sup> So far, only limited kinds of ultrathin inorganic nanostructures such as Au nanowires<sup>1a–c</sup> and metal oxide nanocrystals (NCs) (e.g., TiO<sub>2</sub>, ZnO, Nb<sub>2</sub>O<sub>5</sub>, and rare earth oxides)<sup>1c</sup> have been synthesized by some solution-based structure directing methods. To obtain such ultrathin nanostructures, control of interactions between crystalline seeds and capping surfactant molecules seems to play a crucial role in inducing the rigid anisotropic growth of the NCs along one orientation.<sup>1,2</sup>

Rare earth compound NCs such as oxides,<sup>3a–c</sup> sulfides,<sup>3d</sup> phosphates,<sup>3e</sup> vanadates,<sup>3f</sup> and halides<sup>3g,h</sup> have received extensive attention due to their potential applications in solid-state lasers, optical amplifiers, lighting and displays, and biolabels. It is a big challenge to synthesize various ultrathin rare earth nanostructures via controllable and reproducible solution routes to explore their special material properties (arising from the 4*f* electron configuration) in the sub-2-nm size regime.

In this communication, we report the fluorophilicity-mediated synthesis of highly luminescent self-organized ultrathin EuOF nanowires, with a uniform diameter of ~1.8 nm and length up to several micrometers. The nanowires with a much higher surface Eu<sup>3+</sup> fraction show strong red light emissions with high quantum yields (QYs) of 65% under ultraviolet (UV) light excitations.

Typically, 2 mmol of Eu(CF<sub>3</sub>COO)<sub>3</sub> were added to a mixed solvent composed of 20 mmol of oleic acid (OA) and 20 mmol of oleylamine (OM) at room temperature. The resulting slurry was heated to 100 °C in a vacuum to remove water, thus forming a homogeneous and transparent solution. The resulting mixture was heated to 310 °C under Ar and aged at that temperature for 2 h, resulting in a white colloidal solution. After air cooling, the NCs were precipitated with ethanol and redispersed in cyclohexane.

The broadened peaks on the powder X-ray diffraction (XRD, Rigaku D/MAX-2000) pattern (Figure 1a)<sup>1b,d</sup> and Raman spectrum (Figure S2 in Supporting Information (SI)) indicated the formation of EuOF NCs in a face-centered cubic (fcc) structure (space group: *Fm*3*m*, JCPDS: 26-0635, *a* = 5.53 Å). The inset of Figure 1a showed the small-angle XRD (SAXRD) pattern of the NCs superlattices (SP) formed on a quartz substrate. The series of SAXRD peaks could be assigned to “00*L*” (*L* = 1, 2, 3, 4...) with a layer spacing of 3.0 nm, which corresponded well with the length of the double molecule layer of OA and OM.

The morphologies of the products were observed by the transmission electron microscopy (TEM, FEI Tecnai F30 at an accelerating voltage of 300 kV) at various magnifications. As shown

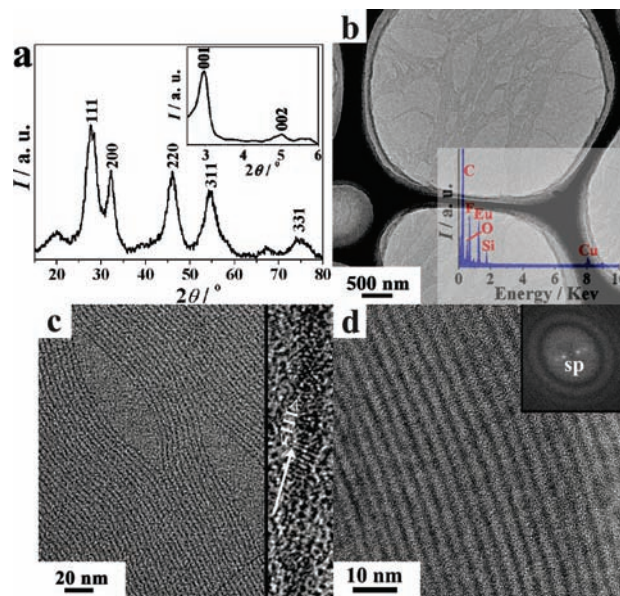


**Figure 1.** (a) Powder XRD pattern of the as-dried EuOF nanowires; inset is the SAXRD pattern of the nanowire superlattices formed on a quartz substrate from a cyclohexane solution. (b) Low magnification TEM image and EDAX spectrum (inset) of ultrathin EuOF nanowires. (c) High magnification TEM image and HRTEM images (inset) of ultrathin EuOF nanowires. (d) TEM image of EuOF nanowire superlattices (SP) via a parallel alignment; inset is the corresponding FFT pattern.

in Figure 1b at a low magnification, the self-organized NC monolayer consisted of well-separated uniform ultrathin nanowires of high aspect ratios (with an average diameter of 1.8 nm and lengths up to several micrometers). The spectrum of energy-dispersive X-ray analysis (EDAX) (inset of Figure 1b) confirmed the formation of the EuOF compound (the atomic ratio of Eu/F = 1.2:1). In addition, these nanowires were frequently looped or bent on the TEM grid (Figure 1c and Figure S3a in SI), indicating that the nanowires were highly flexible and inclined to form crossed networks. High-resolution TEM (HRTEM) measurement demonstrated the presence of both single-crystalline and polycrystalline nanowires, and most of the single-crystalline nanowires grew along the  $\langle 111 \rangle$  direction (inset of Figure 1c and Figure S3b in SI). The polycrystallinity observed for some nanowires might be induced by melting under electron beam irradiation.<sup>1a</sup> The ultrathin EuOF nanowires could spontaneously assemble into 3-D superlattices via a parallel arrangement (Figure 1d) as deposited from the concentrated nanowire dispersion in a mix of cyclohexane and ethanol. The fast Fourier transform (FFT) analysis inserted in Figure 1d indicated that the distance between adjacent nanowires was ~3.0 nm, close to the value calculated from the average double chain length of OA and OM, also in agreement with the SAXRD result.

<sup>†</sup> Peking University.

<sup>‡</sup> Beijing University of Technology.

## Scheme 1. Formation Pathway of Ultrathin EuOF Nanowires

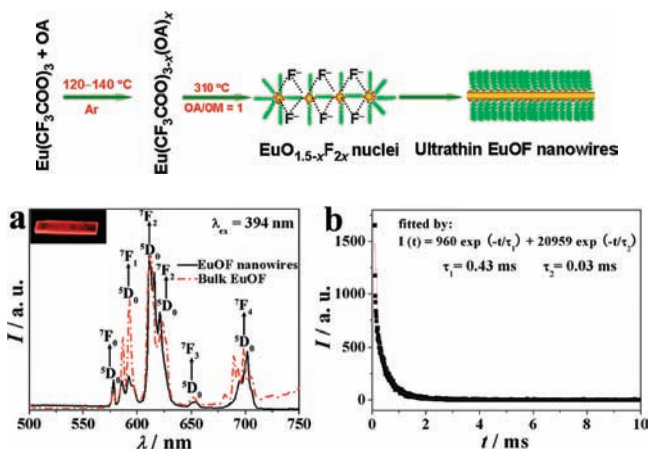


**Figure 2.** (a) Room temperature fluorescence emission spectra of ultrathin EuOF nanowires dispersed in cyclohexane (0.5 wt %) and bulk EuOF powder under  $\lambda_{\text{ex}} = 394$  nm; inset shows a photograph of EuOF nanowire films on a quartz substrate excited with a UV lamp at 254 nm. (b) Luminescence decay curves of the 595 nm emission of  $\text{Eu}^{3+}$  ions in the ultrathin EuOF nanowires under  $\lambda_{\text{ex}} = 394$  nm.

In the synthesis of the ultrathin EuOF nanowires, we found that the  $\text{Eu}(\text{CF}_3\text{COO})_{3-x}(\text{OA})_x$  intermediate ( $x$  denoting the number of OA molecules involved in the reaction) was first generated by the ligand-exchange reaction between  $\text{Eu}(\text{CF}_3\text{COO})_3$  and OA (Figure S4 in SI). The sequential fluorination of the Eu–O bond into the Eu–F bond produced the EuOF nuclei. Further formation of EuOF nanowires was demonstrated to strongly depend on the ratio of OA to OM. When increasing the amount of OA, for example, under OA/OM = 1.5, monodisperse 4.1 nm EuOF spherical NCs were yielded (Figure S5 in SI) as a result of the retarded fluorination by the presence of many free OA ligands; whereas, when increasing the amount of OM (OA/OM < 1),  $\text{Eu}_2\text{O}_3$  NCs rather than EuOF nanowires were readily formed due to the high fluorophilicity of free OM ligands through F–N bonding. Therefore, the ultrathin EuOF nanowires were only formed under OA/OM = 1. At this neutral environment, the reactivity of  $\text{F}^-$  ions produced by the cleavage of the  $\text{Eu}(\text{CF}_3\text{COO})_{3-x}(\text{OA})_x$  intermediate was supposed to be maximized. Therefore, the highest reactivity of  $\text{F}^-$  ions drove the preferred one-dimensional growth of ultrathin EuOF nanowires along the  $\langle 111 \rangle$  direction through the bridging interactions of  $\text{F}^-$  ions among the crystalline seeds (Scheme 1). This nanowire growth mechanism was also confirmed by the time-dependent experimental results. Under OA/OM = 1, as the reaction time went on from 30 min to 1 h, and then to 2 h, the yields of nanowires were significantly enhanced in turn (Figure S6 in SI and Figure 1b). With the same approach, monodisperse sub-2-nm GdOF nanowires in an fcc structure were also obtained under the same conditions (Figure S7 in SI).

Figure 2a depicts the emission spectra of the EuOF nanowires and its bulk counterpart under  $\lambda_{\text{ex}} = 394$  nm (also see Figures S8–10 in SI). The main emission peaks are ascribed to  $\text{Eu}^{3+}$  transitions from  $^5\text{D}_0$  to  $^7\text{F}_j$  ( $J = 0-4$ ), and the intensity ratio of  $^5\text{D}_0 \rightarrow ^7\text{F}_2$  to  $^5\text{D}_0 \rightarrow ^7\text{F}_1$  is equal to the red/orange ( $I_{613}/I_{595}$ ) ratio. The value of  $I_{613}/I_{595}$  of the EuOF nanowires (7.2) is considerably greater than that (2.1) of the bulk counterpart, as a result of the rather large surface  $\text{Eu}^{3+}$  portion in the ultrathin nanostructures (as calculated to be 68.9%; see Figure S1 in SI). The QYs of the as-prepared EuOF nanowires were determined to be as high as 65%, greater than that (39%) of the 4.1 nm EuOF spherical NCs. The nanowire films on a quartz substrate exhibit strong red light under 254 nm

UV excitation (inset of Figure 2a). These results strongly suggest that the concentration quenching of Eu–Eu transitions was markedly restrained due to the presence of dense surface  $\text{Eu}^{3+}$  sites in the ultrathin nanowires as well as the passivation of the surface defects by the capping ligands.<sup>3b,4</sup>

Figure 2b exhibits the luminescence decay curve of the 595 nm emission. The curve can be well fitted using a double exponential function as  $I = I_1 \exp(-t/\tau_1) + I_2 \exp(-t/\tau_2)$  ( $\tau_1, \tau_2$  correspond to the two different lifetimes of  $\text{Eu}^{3+}$  ions). The calculated values for the lifetimes are  $\tau_1 = 0.43$  ms (93%) for the long component and  $\tau_2 = 0.03$  ms (7%) for the short component. The intrinsic  $\text{Eu}^{3+}$  radiative lifetime ( $\tau_C$ ) for the  $^5\text{D}_0 \rightarrow ^7\text{F}_1$  state is calculated by using the formula  $1/\tau_C = A_{\text{MD},0} \times n^3 \times (I_{\text{tot}}/I_{\text{MD}})$ ,<sup>5</sup> where  $n$  is the refractive index of the solvent, equal to 1.43 (cyclohexane);  $A_{\text{MD},0}$  is the spontaneous emission probability for the  $^5\text{D}_0 \rightarrow ^7\text{F}_1$  transition in a vacuum, equal to  $14.65 \text{ s}^{-1}$ ; and  $(I_{\text{tot}}/I_{\text{MD}})$  is the ratio of the total  $\text{Eu}^{3+}$  emission spectrum to the area of the  $^5\text{D}_0 \rightarrow ^7\text{F}_1$  band. The lifetime of  $\tau_C$  is calculated to be 1.4 ms.<sup>5b</sup> On the other hand, the QYs ( $\Phi$ ) can be calculated from the observed luminescence lifetime ( $\tau_{\text{obs}}$ ):  $\Phi_{\text{Eu}} = \tau_{\text{obs}}/\tau_C$ . For the EuOF nanowires, the calculated QY is 33%, lower than the as-measured value (65%).

In conclusion, we have demonstrated the fluorophilicity-mediated synthesis of sub-2-nm EuOF nanowires via the thermolysis of  $\text{Eu}(\text{CF}_3\text{COO})_3$  in a combined solvent of OA and OM. The uniform EuOF nanowires can be parallel aligned on substrates to form superlattices via self-assembly and emit intense  $\text{Eu}^{3+}$  red light under UV light excitation due to the ultrathin nanostructures with surface passivation ligands. This work not only offers a new way for obtaining sub-2-nm sized NCs upon breaking the isotropic growth symmetry via the reactivity control of anions in solutions but also promises new applications such as displays and bioprobes.

**Acknowledgment.** We gratefully acknowledge the financial support from the MOST of China (Grant No. 2006CB601104) and NSFC (Grant Nos. 20871006, 20821091, and 20671005).

**Supporting Information Available:** The synthesis details, structure modeling, and more characterization results about the EuOF nanowires and the bulk EuOF (PDF). This material is available free of charge via the Internet at <http://pubs.acs.org>.

## References

- (a) Lu, X.; Yavuz, M. S.; Tuan, H. Y.; Korgel, B. A.; Xia, Y. *J. Am. Chem. Soc.* **2008**, *130*, 8900. (b) Wang, C.; Hu, Y.; Lieber, C. M.; Sun, S. *J. Am. Chem. Soc.* **2008**, *130*, 8902. (c) Huo, Z.; Tsung, C. K.; Huang, W.; Zhang, X.; Yang, P. *Nano Lett.* **2008**, *9*, 2041. (d) Cademartini, L.; Ozin, G. A. *Adv. Mater.* **2009**, *21*, 1013. (e) Huo, Z.; Tsung, C. K.; Huang, W.; Fardy, M.; Yan, R.; Zhang, X.; Li, Y.; Yang, P. *Nano Lett.* **2009**, *9*, 1260.
- (a) Murray, C. B.; Norris, D. J.; Bawendi, M. G. *J. Am. Chem. Soc.* **1993**, *115*, 8706. (b) Puentes, V. F.; Krishnan, K. M.; Alivisatos, A. P. *Science* **2001**, *291*, 2115. (c) Park, J.; An, K.; Hwang, Y.; Park, J. G.; Noh, H. J.; Kim, J. Y.; Park, J. H.; Hwang, N. M.; Hyeon, T. *Nat. Mater.* **2004**, *3*, 891. (d) Wang, X.; Zhuang, J.; Peng, Q.; Li, Y. D. *Nature* **2005**, *437*, 121. (e) Narayanaswamy, A.; Xu, H. F.; Pradhan, N.; Kim, M.; Peng, X. G. *J. Am. Chem. Soc.* **2006**, *128*, 10310.
- (a) Cao, Y. C. *J. Am. Chem. Soc.* **2004**, *126*, 7456. (b) Si, R.; Zhang, Y. W.; You, L. P.; Yan, C. H. *Angew. Chem., Int. Ed.* **2005**, *44*, 3256. (c) Yu, T.; Joo, J.; Park, Y.; Hyeon, T. *J. Am. Chem. Soc.* **2006**, *128*, 1786. (d) Zhao, F.; Yuan, M.; Zhang, W.; Gao, S. *J. Am. Chem. Soc.* **2006**, *128*, 11758. (e) Lehmann, O.; Kömpe, K.; Haase, M. *J. Am. Chem. Soc.* **2004**, *126*, 14935. (f) Stouwdam, J. W.; Raudsepp, M.; van Veggel, F. C. J. M. *Langmuir* **2005**, *21*, 7003. (g) Sun, X.; Zhang, Y. W.; Du, Y. P.; Yan, Z. G.; Si, R.; You, L. P.; Yan, C. H. *Chem.–Eur. J.* **2007**, *13*, 2320. (h) Du, Y. P.; Zhang, Y. W.; Sun, L. D.; Yan, C. H. *J. Phys. Chem. C* **2008**, *112*, 405.
- (a) Wei, Z. G.; Sun, L. D.; Liao, C. S.; Yan, C. H.; Huang, S. H. *Appl. Phys. Lett.* **2002**, *80*, 1447. (b) Dai, Q.; Song, H.; Wang, M.; Bai, X.; Dong, B.; Qin, R.; Qu, X.; Zhang, H. *J. Phys. Chem. C* **2008**, *112*, 19399.
- (a) Werts, M. H. V.; Jukes, R. T. F.; Verhoeven, J. W. *Phys. Chem. Chem. Phys.* **2002**, *4*, 1542. (b) Vela, J.; Prall, B. S.; Rastogi, P.; Werder, D. J.; Casson, J. L.; Williams, D. J.; Klimov, V. I.; Hollingsworth, J. A. *J. Phys. Chem. C* **2008**, *112*, 20246.

JA9080088